Molecular Insights into the Surface Morphology, Layering Structure, and Aggregation Kinetics of Surfactant-Stabilized Graphene Dispersions

Shangchao Lin,[†,‡,§] Chih-Jen Shih,[†,§] Michael S. Strano,[†] and Daniel Blankschtein[†,*]

[†]Departments of Chemical and [‡]Mechanical Engineering, Massachusetts Institute of Technology, Cambridge, Massachusetts 02139

*Corresponding author. Phone: (617) 253-4594. Fax: (617) 252-1651. E-mail: dblank@mit.edu.

[§]These authors contributed equally to this work.

Supporting Materials

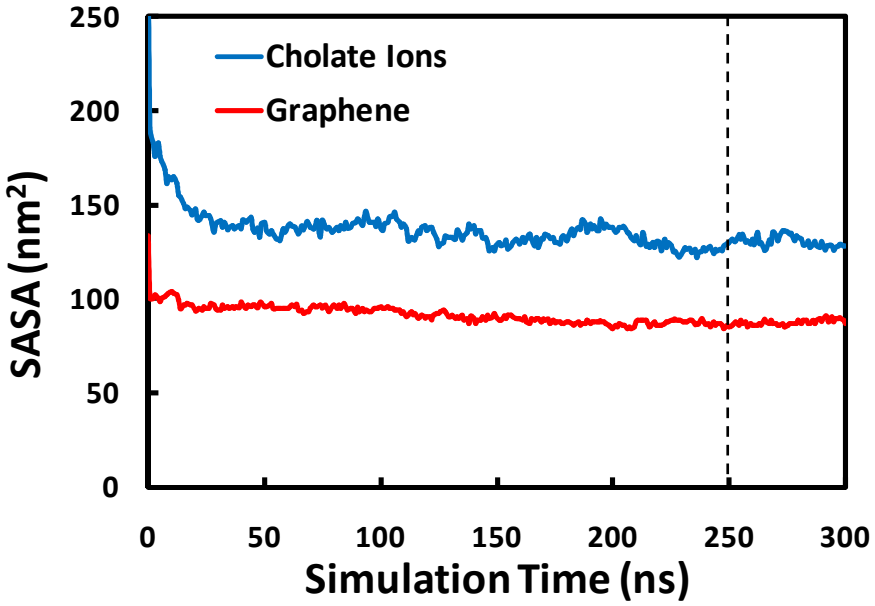

Figure S1. Solvent accessible surface areas (SASAs) of a graphene monolayer and the cholate ions, monitored as a function of simulation time. As shown, the fluctuations in the SASA curves are significant at the beginning, and are dampened after about 200 ns, indicating that the system has reached equilibrium. Therefore, data analysis was performed during the last 50 ns of the entire simulation run, as indicated by the time period beyond the vertical dashed line.

Table S1: Summary of the Simulated Systems.

System	Number of Graphene Sheets	Number of SC Molecules	Number of Water Molecules	Total Number of Atoms	Simulation Box Size [c] (nm^3)	Simulation Time (ns)
1 [a]	1	56	10,981	38,967	7.38 x 7.67 x 6.69	300 ns
2-52 [b]	2	112	14,000	54,048	8.74 x 8.74 x 6.80	20 ns each

[a] Sodium cholate adsorption and surface self-assembly simulations on a graphene monolayer.

[b] Potential of mean force (PMF) simulations at 51 intersheet separations between two parallel graphene-SC assemblies.

[c] Averaged over the production run of the simulation with small fluctuations from the pressure coupling.

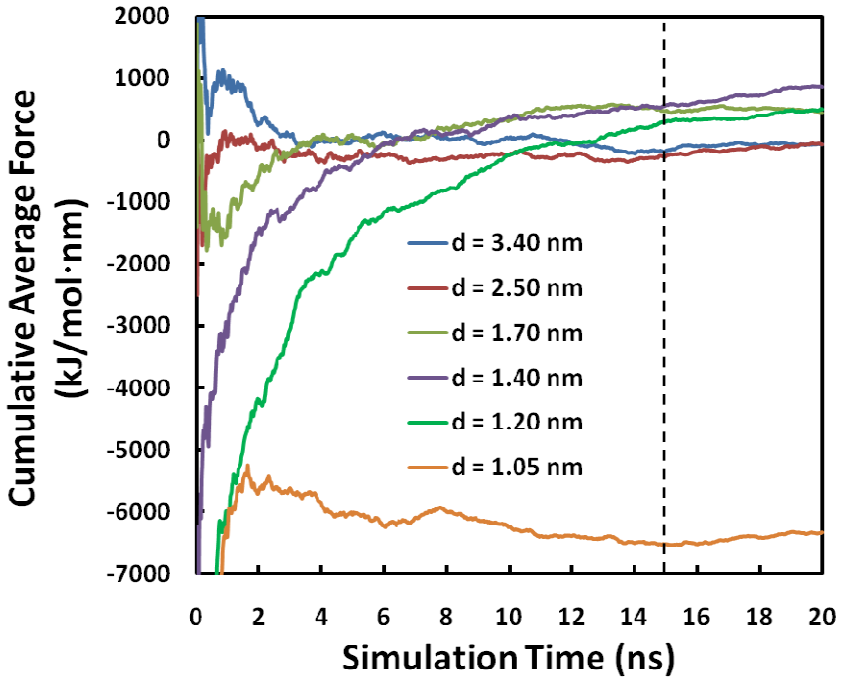

Figure S2. Cumulative average forces as a function of simulation time at several selected inter-sheet separations, *d*. As shown, the fluctuations in the force curves are significant at the beginning, and are dampened after about 10 ns, indicating that the system has reached equilibrium. Therefore, data analysis was performed during the last 5 ns of each simulation run, as indicated by the time period beyond the vertical dashed line.

S1: Summary of Experimental Procedures

Briefly, the bilayer-enriched graphene dispersion in aqueous SC solutions was prepared using Stage-2 GICs, as demonstrated in our recent report.[1] HOPG was chosen as a high-quality graphite source, and we used the halogen intercalant ICl to form Stage-2 ionic GIC. In this scheme, Stage-2 GICs have every 2nd layer of the graphite lattice intercalated. The Stage-2 GICs were first treated to yield expanded graphite (EG) by removing the ICl intercalant during the "thermal shock". The foam-like EG was then immersed in 2 wt% SC aqueous solutions and subjected to slow homogenization (6,800 rpm, 30 minutes), mild sonication (40 kHz, 10 minutes), and centrifugation (2,000 rpm, 805 g, 20 minutes) to yield clear and grey dispersions. In order to locate and isolate large flakes from poly-disperse graphene solutions for further characterization, an on-chip separation method based on size utilizing the "coffee-ring effect" was used.[2] Using this method, the graphene flakes are separated based on the lateral size but independently of their thickness on a SiO_2-Si substrate. Raman spectroscopy was used to characterize the isolated graphene flakes deposited on the substrate. The 2D peak corresponding to specific numbers of stacked layers in our exfoliated graphene flakes exhibits the same layering dependence as that observed in micromechanically-cleaved graphene on the same substrate,[3] indicating that the solution processed graphene flakes are AB-stacked.[1] Systematic statistical analysis of the initial thickness (or layer number) distributions for large graphene flakes was carried out using a combination of optical microscopy and Raman spectroscopy.

The Lambert-Beer plot of graphene-SC solutions was calibrated using graphite flakes as raw materials (see Figure 6A). Graphene solutions were prepared by adding 1.5 g of natural graphite flakes (Sigma-Aldrich 332461) to 150 mL of 20 mg/mL sodium cholate aqueous solution in a 200 mL capped round-bottomed flask. Sonication was carried out in a sonication bath (VWR Aquasonic model 50D) for 30 minutes. After sonication, the sample was extracted from the flask into three centrifuge tubes (Falcon 50 mL polypropylene conical tubes), and left to stand overnight to allow thick graphite flakes to sediment out of the solution. The samples were then centrifuged for 30 minutes at 4000 rpm (990 g) in a Hettich Universal 320 centrifuge. After centrifugation, the top half of the dispersion was extracted by vacuum pipette (~8 mL) and retained for use. A 10 mL of the graphene solution was diluted sequentially with the 20 mg/mL SC solution to obtain solutions at 6 different graphene concentrations. The original and the

diluted solutions were decanted into 6 quartz cuvettes, and the optical absorbance was measured using a UV/visible spectrophotometer (Beckman Coulter DU800).

The graphene concentration of the original solution was obtained by vacuum filtering the solution (50 – 65 mL) through three layers of Millipore nitrocellulose membranes (~0.45 μm pore size and 0.47 mm membrane diameter). After filtration, the membranes were rinsed with 100 mL Milli-Q water for ten times to get rid of the residue surfactants, and subsequently dried under room temperature overnight. The weight of the membranes before and after filtration was measured using a microbalance.

S2: Kinetic Theory of Graphene Aggregation

To utilize the simulated PMF curve (see Figure 4A) in the theoretical model, the first step involves fitting the PMF curve to a semi-empirical analytical model. To capture the primary features of the PMF curve, we propose the following model to describe the PMF per unit area, Φ, between two parallel graphene sheets with an intersheet separation, d:

$$\Phi(d) = \varepsilon\left[\left(\frac{r_0}{d}\right)^{12} - 2\left(\frac{r_0}{d}\right)^{6}\right] + \beta_1 \exp\left[-\frac{(d-r_1)^2}{2\sigma_1^2}\right] + \beta_2 \exp\left[-\frac{(d-r_2)^2}{2\sigma_2^2}\right] + \alpha \exp\left[-\kappa(d-r_3)\right] \quad \text{(S1)}$$

where ε and r_0 are the well-known parameters in the Lennard-Jones (LJ) potential that characterize the depth and location, respectively, of the metastable energy well; β_1, r_1, and σ_1 characterize the height, location, and width, respectively, of the primary energy barrier; β_2, r_2, and σ_2 characterize the height, location, and width, respectively, of the small, secondary energy barrier; and α, κ, and r_3 characterize the magnitude, decay rate, and location of the long-range repulsive electrostatic potential between the two SC-covered graphene sheets (see Figure 4A). Note that to account for the electrostatic interactions present in the case of SC-covered graphene dispersions considered here, we modified Eq. (1) of ref.,[4] which results in Eq. (S1) used here. The parameters in Eq. (S1) were obtained by least-square fitting of Eq. (S1) to the simulated PMF curve in Figure 4A, and are summarized in Table S2.

Table S2: Summary of Fitted Parameters in Eq. (S1). Note that ε, β_1, β_2, and α are in units of kJ/mol·nm^2, r_0, r_1, σ_1, r_2, σ_2, and r_3 are in units of nm, and κ is in units of nm^{-1}.

ε	r_0	β_1	r_1	σ_1	β_2	r_2	σ_2	α	κ	r_3
46.27	1.05	16.77	1.20	0.10	4.23	1.46	0.08	13.29	2.74	1.43

Our kinetic model considers individually-suspended graphene sheets in a solution media, and makes the following assumptions:[4] (i) the aggregation process is diffusion controlled, (ii) since the graphene sheets can translate freely, they are modeled as effective spheres, (iii) the lateral size of all graphene sheets is the same, (iv) the estimated diffusivity of graphene sheets, $D = 10^{-12}$ m^2/s, is independent of its layer number, i, since the friction factor in the Stokes-Einstein relation depends primarily on the lateral size of a graphene sheet,[5] (v) the graphene sheets aggregate and precipitate when the number of stacking layers exceeds the maximum number of graphene sheet layers which exist in a solution phase stably, M = 10,[4] and (vi) due to the relatively negligible thickness of the graphene sheets, the intersheet interaction potential energy is assumed to be independent of the number of layers in the two sheets.

Considering all possible collisions (reaction pairs), the time-dependent number concentration (in 1/m^3) of monolayer graphene, $N_1(t)$, as a function of time is given by the following consumption term:[4]

$$\frac{dN_1(t)}{dt} = -\sum_{i=1}^{\mathrm{M}} kN_1(t)N_i(t) \tag{S2}$$

where $N_i(t)$ is the time-dependent number concentration of i-layer graphene, and k is the reaction rate constant (i.e., the rate constant of aggregation in the present study). Similarly, the time-dependent number concentration of bilayer graphene, $N_2(t)$, is modeled as the sum of the source and consumption terms. Specifically,

$$\frac{dN_2(t)}{dt} = kN_1(t)N_1(t) - \sum_{i=1}^{\mathrm{M}} kN_2(t)N_i(t) \tag{S3}$$

More generally, beginning with trilayer graphene, the time-dependent number concentration of m-layer graphene, $N_m(t)$ $(3 \le m \le \mathrm{M})$, is modeled as the sum of the relevant source and consumption terms. Specifically,

$$\frac{dN_m(t)}{dt} = \frac{1}{2}\sum_{i=1}^{m-1} kN_i(t)N_{m-i}(t) - \sum_{i=1}^{M} kN_i(t)N_m(t) \tag{S4}$$

where the factor of 1/2 avoids counting the same collision twice in the source term. The rate constant of aggregation, k, can be expressed as follows:[4]

$$k = \frac{8\pi D}{\int_{r_0}^{\infty} \frac{\exp[V(r)/k_B T]}{r^2} dr} \tag{S5}$$

where r is the effective distance between two graphene sheets, r_0 = 1.05 nm is the distance of closest approach at the metastable state, and $V(r)$ is the intersheet interaction potential energy (see below). It is noteworthy that when two graphene sheets approach, all collision angles and areas are possible. Irrespectively of the collision angle, the graphene sheets need to overcome the dominant energy barrier resulting from the last layer of confined molecules which includes cholate ions and sodium counterions, as discussed in Section 3.4. Therefore, the ensemble average of all collision angles can be viewed as an effective face-to-face collision that we have considered in our analysis, where the radial coordinate, r, corresponds to the intersheet separation, d, in our MD simulations. Consequently, the intersheet interaction potential energy, $V(d)$, was further simplified as follows:

$$V(d) = \Phi(d) \times A_C \tag{S6}$$

where $\Phi(d)$ is the PMF between two parallel graphene sheets per unit area obtained utilizing our MD simulations (see Figure 4A), and A_C is the average collision area, which is the *single adjustable parameter* in our kinetic model. For given values of the parameter, A_C, and the initial number concentrations of the various graphene layer types, N_{i0}, the time-dependent number concentration of various graphene layer types, $N_i(t)$, can be obtained by simultaneously solving Eqs. (S1)–(S6) numerically.

References

(1) Shih, C.-J.; Vijayaraghavan, A.; Krishnan, R.; Sharma, R.; Han, J.-H.; Ham, M.-H.; Jin, Z.; Lin, S.; Paulus, G. L. C.; Reuel, N. F.; Wang, Q. H.; Blankschtein, D.; Strano, M. S. *Nature Nanotechnology* **2011**, *6*, 439-445.

(2) Deegan, R. D.; Bakajin, O.; Dupont, T. F.; Huber, G.; Nagel, S. R.; Witten, T. A. *Nature* **1997**, *389*, 827-829.

(3) Ferrari, A. C.; Meyer, J. C.; Scardaci, V.; Casiraghi, C.; Lazzeri, M.; Mauri, F.; Piscanec, S.; Jiang, D.; Novoselov, K. S.; Roth, S.; Geim, A. K. *Physical Review Letters* **2006**, *97*, 187401.

(4) Shih, C.-J.; Lin, S.; Strano, M. S.; Blankschtein, D. *Journal of the American Chemical Society* **2010**, *132*, 14638-14648.

(5) Hiemenz, P. C.; Rajagopalan, R. *Principles of colloid and surface chemistry*; 3rd ed.; Marcel Dekker: New York, 1997.

Complete ref. 8:

Hernandez, Y.; Nicolosi, V.; Lotya, M.; Blighe, F. M.; Sun, Z. Y.; De, S.; McGovern, I. T.; Holland, B.; Byrne, M.; Gun'ko, Y. K.; Boland, J. J.; Niraj, P.; Duesberg, G.; Krishnamurthy, S.; Goodhue, R.; Hutchison, J.; Scardaci, V.; Ferrari, A. C.; Coleman, J. N. *Nature Nanotechnology* **2008**, *3*, 563-568.